satisfactory on a qualitative basis. A detailed quantitative verification (not presented here) can only be achieved within certain bounds because of: (1) Assumption 2 in Section 2 and other assumptions like Gaussian distribution of $q_i$'s in the algorithm development in Section 3; and (2) uncertainties in the selection of parameters like mean $\theta$ for computing the detection threshold $\sigma$. However, there is no approximation involved in the analytical derivation in Section 2.

## 5 Summary and Conclusions

The multiple-level hypotheses test algorithm, presented in this paper, is not restricted to any specific structure of measurement noise statistics. Its computational efficiency is enhanced if the noise distribution in the parity vector, generated from a linear combination of redundant measurements, is assumed to be Gaussian. The algorithm has been implemented on a commercially available microcomputer, and then tested for on-line detection of faulty sensors in a nuclear research reactor. This fault detection procedure is particularly suitable for intelligent instrumentation in continuous processes like spacecraft, aircraft, and nuclear power plants where redundant measurements are usually available for critical plant variables. Further research is recommended to quantify the accuracy and robustness of multi-level fault detection test procedures for different types of processes.


## Acknowledgment

The author acknowledges the benefits of discussion with Dr. M. Desai and the assistance offered by the staff of the MIT Nuclear Reactor Laboratory for conducting the experiments.


## References


1 Ray, A., "Fault Detection in Multiply-Redundant Measurement Systems via Sequential Testing," ASME Journal of Dynamic Systems, Measurement, and Control, June 1989, pp 329-332.

2 Chien, T. T., and Adams, M. B., "A Sequential Failure Detection Technique and its Application," *IEEE Trans. Aut. Contr.*, Vol. AC-21, No. 5, Oct. 1976, pp. 750-757.

3 Chien, T. T., "An Adaptive Technique for a Redundant-Sensor Navigation Systems," *C. S. Draper Laboratory* Report No. T-560, Feb. 1972.

4 Ray, A., and Desai, M., "A Redundancy Management Procedure for Fault Detection and Isolation," ASME Journal of Dynamic Systems, Measurement, and Control, Sept. 1986, pp. 248-254.

5 Ray, A., and Desai, M., "A Calibration and Estimation Filter for Multiply Redundant Measurement Systems," ASME Journal of Dynamic Systems, Measurement, and Control, June 1984, pp. 149-156.

6 *Reactor Systems Manual*, Report No. MITNRL-004, MIT Nuclear Reactor Laboratory, 1980.


# On Modeling of Integrated Communication and Control Systems[1]


**Luen-Woei Liou[2] and Asok Ray[2]**



*In a two-part paper [1,2], Ray and Halevi reported modeling of Integrated Communication and Control Systems (ICCS). Varying and distributed delays are introduced in the control system due to asynchronous time-division multiplexing in the communication network. This correspondence illustrates the relationship of Ray and Halevi's approach to that of Kalman and Bertram [3] under nonsynchronous sampling.*


## Nomenclature

- $A$ = plant system matrix $(n \times n)$
- $A_s$ = plant state transition matrix $(n \times n)$
- $B$ = plant input matrix $(n \times m)$
- $C$ = plant output matrix $(r \times n)$
- $F$ = controller system matrix $(q \times q)$
- $G$ = controller input matrix $(q \times r)$
- $H$ = controller output matrix $(m \times q)$
- $J$ = controller direct coupling matrix $(m \times r)$
- $l$ = maximum # of delayed actuator commands in one sampling period
- $p$ = maximum delay (# of samples) for sensor data arrival
- $T$ = nominal sampling period for the sensor and controller
- $T_c$ = controller sampling period
- $T_s$ = sensor sampling period
- $u$ = plant input vector $(m \times 1)$
- $X$ = augmented state vector $((n+q+m) \times 1)$
- $x$ = plant state vector $(n \times 1)$
- $y$ = plant output vector, i.e., generated sensor data $(r \times 1)$
- $\Delta_s$ = time skew between sensor and controller sampling instants
- $\delta_{ca}$ = controller-to-actuator data latency
- $\delta_p$ = processing delay at the controller computer
- $\delta_{sc}$ = sensor-to-controller data latency
- $\eta$ = controller state vector $(q \times 1)$
- $\Theta_{sc}$ = sensor-controller delay
- $\Theta_{ca}$ = controller-actuator delay
- $\Phi$ = augmented system matrix

## 1 Introduction

Varying and distributed delays are introduced in Integrated Communication and Control Systems (ICCS) due to asynchronous time-division multiplexing in the network [1, 2]. The finite-dimensional modeling of systems with varying and distributed delays, reported by Ray and Halevi [1, 2], uses the concept of state transition to transform the continuous-time model into a discrete-time form. In 1959, Kalman and Bertram [3] used this technique to provide a unified approach for modeling different types of sampled data systems that are not subjected to any induced delays. The objective of this correspondence is to illustrate the relationship between these two modeling approaches.


[1]This work was supported in part by Office of Naval Research grant No. N00014-90-J-1513; NASA Lewis Research Center grant No. NAG 3-823; National Science Foundation Research grant No. DMC-8707648.



[2]Mechanical Engineering Department, The Pennsylvania State University, University Park, PA 16802. Prof. Ray is a Mem. ASME.



Contributed by the Dynamic Systems and Control Division of The American Society of Mechanical Engineers. Manuscript received by the Dynamic Systems and Control Division May 1989; revised manuscript received October 1989. Associate Editor: D. Hrovat.

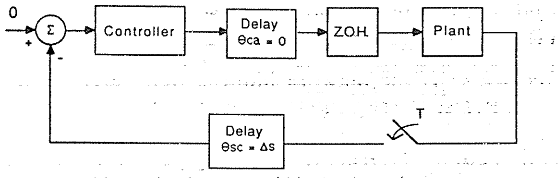


Fig. 1 Schematic diagram for the delayed control system

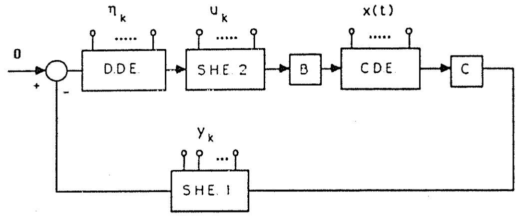


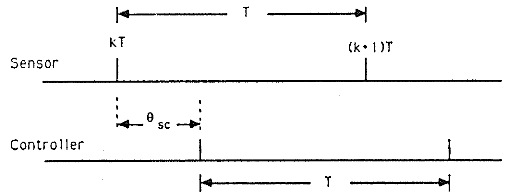


Fig. 2 Schematic diagram for nonsynchronous sampling

## 2 Comparison of the Modeling Approaches: Zero Data Latency

This section compares the modeling approaches, proposed in [1, 2] and [3], for modeling *ICCS* under the conditions of: (i) identical sampling intervals for the sensor and controller, i.e., $T_s = T_c = T$, and (ii) negligible network traffic, i.e., the induced data latencies $\delta_{sc}$ and $\delta_{ca}$ (see Section 3 of [1] and also the Nomenclature) are both equal to 0, and (iii) negligible data processing delay at the controller, i.e., $\delta_p \approx 0$. Then, the network-induced delays reduce to:

$$\Theta_{sc} = \Delta_s \text{ and } \Theta_{ca} = 0. \tag{1}$$

*Remark 1*: If the processing delay $\delta_p$ is a constant, there is no loss of generality in assuming $\delta_p = 0$ because $\delta_p$ can be lumped with the time skew $\Delta_s$. This follows directly from Proposition A.1 in Appendix A of [1]. ■

If the instants of sensor and controller samplings are synchronized, i.e., time skew $\Delta_s = 0$, then the problem reduces to a conventional sampling system, and both models are trivially identical. Therefore, we consider the general case of *nonsynchronous sampling* [3], i.e., the instants of sensor and controller sampling are not synchronous, implying that $\Delta_s \in (0, T)$. Since the network-induced delays, $\Theta_{sc}$ and $\Theta_{ca}$ are constant by equation (1), the augmented system matrix $\Phi_k$ in [1, 2] (see equation (4.11) in [1]) becomes time-invariant.

To elucidate similarities between the modeling approaches of [1, 2] and [3], we consider a single loop feedback control system where the continuous state equation of the plant and the discrete controller state equation are given as:

$$\textit{Plant:} \qquad dx(t)/dt = Ax(t) + Bu(t) \tag{2}$$

$$y(t) = Cx(t)$$

$$\textit{Controller:} \qquad \eta_{k+1} = F\eta_k - Gy_k \tag{3}$$

$$u_k = H\eta_k - Jy_k$$

where $x \in \mathcal{R}^n$, $\eta \in \mathcal{R}^q$, $y \in \mathcal{R}^r$, and $u \in \mathcal{R}^m$, and the matrices $A$, $B$, $C$, $F$, $G$, $H$, and $J$ are of compatible dimensions.

Figure 1 exhibits the delayed control system structure considered by Ray and Halevi [1, 2] with network-induced delays defined in (1). The control commands, $u_k$ and $u_{k-1}$ act upon the actuator during the $k$th sampling period, i.e., $\ell = 1$. Also, the delay (in # of samples) of arrival of the sensor data at the controller, $p(k) = 0 \, \forall k$. Under these conditions, equation (4.11) of [1] reduces to

$$X_{k+1} = \Phi x_k \tag{4}$$

where $X_k = [x_k{}^T \eta_k{}^T u_{k-1}{}^T]^T$ is the augmented state vector,

$$\Phi := \begin{bmatrix} A_s - B_0 JC & B_0 H & B_1 \\ -GC & F & 0 \\ -JC & H & 0 \end{bmatrix}, \; A_s := \exp(AT),$$

$$B_1 := \int_0^{\Theta_{sc}} \exp(A[T-\sigma]) \, d\sigma \, B,$$

$$\text{and } B_0 := \int_{\Theta_{sc}}^{T} \exp(A[T-\sigma]) \, d\sigma \, B.$$

*Remark 2*: The matrices $\Phi$, $B_1$ and $B_0$ are time-varying in general [1]. However, for zero (in fact, any constant) data latency, these matrices are constant. ■

Now we proceed to show that results, identical to those derived from (4), can be obtained by using the approach of Kalman and Bertram [3]. Figure 2 follows [3] to present the layout of individual dynamical elements where CDE refers to the continuous dynamical element, i.e., the plant, DDE refers to the discrete dynamic element, i.e., the digital controller, and SHEs refer to the sample and hold element, i.e., ideal sampler and zero order hold.

For the convenience of formulating the transition matrices of the individual blocks in Fig. 2, the augmented state vector is selected as $X_k' = [x_k{}^T \, y_{k-1}^T \, \eta_k^T \, u_{k-1}^T]^T$. It is to be noted that $X_k'$ is different from $X_k$ in (4) in the sense that $y_{k-1}$ is included in $X_k'$. The transition matrices are defined below.

Sample and hold element 1 (SHE1):

$$S_1 = \begin{bmatrix} I_n & 0 & 0 & 0 \\ C & 0 & 0 & 0 \\ 0 & 0 & I_q & 0 \\ 0 & 0 & 0 & I_m \end{bmatrix} \tag{5}$$

Discrete dynamic element (DDE):

$$D_1 = \begin{bmatrix} I_n & 0 & 0 & 0 \\ 0 & I_r & 0 & 0 \\ 0 & -G & F & 0 \\ 0 & 0 & 0 & I_m \end{bmatrix} \tag{6}$$

Sample and hold element 2 (SHE2):

$$S_2 = \begin{bmatrix} I_n & 0 & 0 & 0 \\ 0 & I_r & 0 & 0 \\ 0 & 0 & I_q & 0 \\ 0 & -J & H & 0 \end{bmatrix} \tag{7}$$

For the continuous dynamic element (CDE), defined in (2), the states at an instant $t$ for a constant control effort $u_0$ in the interval $(t_0, t)$ is given as:

$$x(t) = \exp\,(A[t-t_0])\, x(t_0) + \int_0^{t-t_0} \exp(A[t-t_0-\sigma])\, B \, d\sigma \, u_0 \tag{8}$$

The transition matrix of CDE follows from (8).

$$\phi(\tau)=\begin{bmatrix} \exp(A\tau) & 0 & 0 & B(\tau) \\ 0 & I_r & 0 & 0 \\ 0 & 0 & I_q & 0 \\ 0 & 0 & 0 & I_m \end{bmatrix} \tag{9}$$

where $\tau$ is the interval between two instants of transitions, and

$$B(\tau):=\int_0^\tau \exp\,(A[\tau-\sigma])\,d\sigma\,B=\int_0^\tau \exp(A\sigma)\,d\sigma\,B.$$

Following the approach of Kalman and Bertram [3], the composite state transition matrix is generated as a product of individual transition matrices from (5), (6), (7), and (9) as follows.

At the instant $kT$, sensor samples the plant output $y_k$. This changes the augmented state vector from $X_k'$ to $S_1X_k'$. From the instant $kT^+$ to the instant $kT+\Theta_{sc}$, only the continuous plant changes its state. Therefore, the augmented state at $(kT+\Theta_{sc})^-$ is $\phi(\Theta_{sc})S_1X_k'$. Since the processing delay $\delta_p$ at the controller is assumed to be negligible [or it is lumped with $\Theta_{sc}$ (see Remark 1)], two state transitions take place at the instant $kT+\Theta_{sc}$. The first transition follows from the controller output equation (3) where the control command $u_k$ depends on $\eta_k$ and $y_{k-1}$. Therefore, the augmented state, viewed at the actuator at the instant $(kT+\Theta_{sc})^+$ is $S_2\phi(\Theta_{sc})\,S_1X_k'$. The second transition takes place as the controller changes its state which causes the augmented state to be $DS_2\phi\;(\Theta_{sc})S_1X_k'$ at $(kT+\Theta_{sc})^+$. Finally, from the instant $(kT+\Theta_{sc})^+$ to the instant $(k+1)T$, *CDE* changes the augmented state to yield the following state transition relationship.

$$X_{k+1}'=\Phi' X_k' \tag{10}$$

where $\Phi':=[\phi(T-\Theta_{sc})\;D\;S_2\phi(\Phi_{sc})S_1]$

The composite state transition matrix $\Phi'$ is simplified using (5), (6), (7), and (9) as follows.

$$\Phi'=\begin{bmatrix} A_s-B(T-\Theta_{sc})JC & 0 & B(T-\Theta_{sc})H & \exp\,(A[T-\Theta_{sc}])B(\Theta_{sc}) \\ C & 0 & 0 & 0 \\ -GC & 0 & F & 0 \\ -JC & 0 & H & 0 \end{bmatrix} \tag{11}$$

where $A_s:=\exp(AT)$ as defined in (4) and the terms involving $B(\cdot)$ are simplified as follows.

$$\mathrm{B}(\mathrm{T}-\Theta_{sc})=\int_0^{T-\Theta_{sc}}\exp(A[T-\Theta_{sc}-\sigma])\;d\sigma\;B$$

$$=\int_{\Theta_{sc}}^{T}\exp(A[T-\sigma])\;d\sigma\;B=B_0,$$

and $\exp(A[T-\Theta_{sc}])\;B(\Theta_{sc})$

$$=\exp(A[T-\Theta_{sc}])\times$$

$$\int_0^{\Theta_{sc}}\exp(A[\Theta_{sc}-\sigma])\;d\sigma\;B$$

$$=\int_0^{\Theta_{sc}}\exp(A[T-\sigma])\;d\sigma\;B=B_1.$$

*Remark 3*: Since $B(T)=B_0+B_1$, it follows from (9) that

$$\phi(T-\tau)\phi(\tau)=\phi(T)\quad\forall\tau\epsilon(0,T)\;\blacksquare$$

The second column in the matrix $\Phi'$ is **0** and this corresponds to the second (vector) element $y_{k-1}$ in the augmented state vector $X_k'=[x_k^T y_{k-1}{}^T\eta_k^T u_{k-1}{}^T]^T$. If this redundant information (which is available as $y_{k-1}=C\,x_{k-1}$ from the plant model in (2) and also from the second row of $\Phi'$ in (11)) is eliminated, then $X_k'$ reduces to $X_k$ in (4). Accordingly, by deleting the second column and second row of $\Phi'$, (11) becomes identical to (4).

*Remark 4*: If the network-induced data latencies are constant, then also the two modeling approaches would yield identical results. In that case the augmented state vector $X_k$ may contain additional terms representing past values of $y$ and $u$. Following Remark 4.4 of [1], $y_{k-i}$ can always be replaced by $u_{k-l-i}$ as part of the state vector but the converse is true only if the controller matrix $F$ is invertible. Thus the restriction of zero latency can be relaxed to constant data latency. ■

Next we show how the additional book keeping needed to keep track of varying delays would complicate the modeling task if the approach of Kalman and Bertram is used.

## 3 Impact of Varying Data Latencies on Modeling of ICCS

Varying sensor-to-controller data latency, $\delta_{sc}^j$, influences the sensor-controller delay, $\Theta_{sc}^j$, under nonsynchronous sampling (i.e., identical sensor and controller sampling period, $T$, and a nonzero skew $\Delta_s$ between their sampling instants) in the following way [1]:

$$\Theta_{sc}^j=kT+\Delta_s\text{ for }(k-1)T+\Delta_s\le\delta_{sc}{}^j<kT+\Delta_s \tag{12}$$

The above phenomenon is likely to disorder the sequence of events at the controller and the actuator. For example, a sensor data can arrive before or after a given controller sampling instant depending on the magnitude of $\delta_{sc}$.

We now proceed to illustrate the impact of the phenomenon in (12) for the case of nonsynchronous sampling under the restriction of the data latencies being bounded within the interval $[0,T]$ with probability 1. Figure 3 shows a timing diagram to explain the impact of $\delta_{sc}$ on the sequence of events at the controller. In view of the fact that the time skew $\Delta_s$ is always bounded between 0 and $T$, there are four possible scenarios at each sampling period as listed below.

1. If $\delta_{sc}<\Delta_s$ and $\Theta_{ca}^k+\Delta_s<T$, then the event sequence is unaltered, i.e., similar to that if $\delta_{sc}=\delta_{ca}=\delta_p=0$. (Note that $\theta_{ca}:=\delta_{ca}+\delta_p$.) Then, $y_k$ is used in computing $u_k$ which arrives at the actuator during the $k^{\text{th}}$ sampling period, and this $u_k$ is used for generating $x_{k+1}$. However, the elements $B_0$ and $B_1$ in $\Phi$ in (4) will have to be changed because the limits of integration would be different due to the introduction of varying $\delta_{ca}$. (See equation (4.5) in [1].)
2. If $\delta_{sc}\ge\Delta_s$ and $\Theta_{ca}^k+\Delta_s<T$, then the sensor data, $y_k$, arrives at the controller after the $k^{\text{th}}$ sampling instant. Therefore, $y_k$ cannot be used in computing $u_k$, and this causes the event sequence to be altered. However, $u_k$ arrives at the actuator within the $k^{\text{th}}$ sampling period.
3. If $\delta_{sc}<\Delta_s$ and $\Theta_{ca}^k+\Delta_s\ge T$, then $y_k$ is used in computing $u_k$. Since this $u_k$ does not arrive at the actuator within the $k^{\text{th}}$ sampling period, the event sequence is altered.
4. If $\delta_{sc}\ge\Delta_s$ and $\Theta_{ca}^k+\Delta_s\ge T$, then both the above disorderly phenomena take place, and consequently the event sequence is altered.

The above four scenarios would occur randomly in the event of stochastically varying data latencies, which usually happens in *ICCS*.

In order to deal with the above complexity of varying latencies, a concept of event tracking has been introduced by

Ray and Halevi [1, 2] by systematically taking into account the sequences of arrival time $\{t_k\}$ and event indicator $\{p(k)\}$. Some of the elements of the augmented state transition matrix, $\Phi_k$, of a control system in *ICCS* are functions of $\{t_k\}$ and $\{p(k)\}$, and its structure remains invariant for all scenarios. In contrast, Kalman and Bertram's approach would require a significant amount of book-keeping when applied to varying data latencies. Incorporation of this concept of event tracking in Kalman and Bertram's approach is not a straight-forward task because alterations in the event sequence would change the order of multiplications of the individual sub-state-transition matrices. For $\delta_{sc}^k < T\,\forall k$, and $\delta_{sc}^k \ge \Delta_s$ and/or $(\Theta_{ca}{}^k + \Delta_s) \ge T \ge T$ for some $k$, the system state may have to be augmented as:

$$X'_k = x_k^T\, y_{k-1}^T\, y_{k-2}^T\, \eta_k^T\, u_{k-1}^T\, u_{k-2}^T]^T$$

and the matrices $S_1$, $D$, $S_2$, and $\phi$ need to be modified as:

$$S_1 = \begin{bmatrix} I_n & 0 & 0 & 0 & 0 & 0 \\ C & 0 & 0 & 0 & 0 & 0 \\ 0 & I_r & 0 & 0 & 0 & 0 \\ 0 & 0 & 0 & I_q & 0 & 0 \\ 0 & 0 & 0 & 0 & I_m & 0 \\ 0 & 0 & 0 & 0 & 0 & I_m \end{bmatrix}$$

$${}^pD = \begin{bmatrix} I_n & 0 & 0 & 0 & 0 & 0 \\ 0 & I_r & 0 & 0 & 0 & 0 \\ 0 & 0 & I_r & 0 & 0 & 0 \\ 0 & -G(1-p) & -G_p & F & 0 & 0 \\ 0 & 0 & 0 & 0 & I_m & 0 \\ 0 & 0 & 0 & 0 & 0 & I_m \end{bmatrix}$$

$${}^pS_2 = \begin{bmatrix} I_n & 0 & 0 & 0 & 0 & 0 \\ 0 & I_r & 0 & 0 & 0 & 0 \\ 0 & 0 & I_r & 0 & 0 & 0 \\ 0 & 0 & 0 & I_q & 0 & 0 \\ 0 & -J(1-p) & -Jp & H & 0 & 0 \\ 0 & 0 & 0 & 0 & I_m & 0 \end{bmatrix}$$

$${}^\theta\phi(\tau) = \begin{bmatrix} \exp(A\tau) & 0 & 0 & 0 & (1-\theta)B(\tau) & \theta B(\tau) \\ 0 & I_r & 0 & 0 & 0 & 0 \\ 0 & 0 & I_r & 0 & 0 & 0 \\ 0 & 0 & 0 & I_q & 0 & 0 \\ 0 & 0 & 0 & 0 & I_m & 0 \\ 0 & 0 & 0 & 0 & 0 & I_m \end{bmatrix}$$

where $p\in\{0,1\}$ and $\theta\in\{0,1\}$ represent number of sampling periods by which the arriving data is delayed at the controller and actuator, respectively. Following the notations used in (10), the disorder in event sequence at the $k^{\text{th}}$ sample is illustrated by using the four scenarios that are described earlier. In the examples to follow for each of the four scenarios, two cases are considered on the basis of arrival instant of the control signal $u_{k-1}$ at the actuator: *Case 1*: $(\Theta_{ca}^{k-1} + \Delta_s) < T$, i.e., $u_{k-1}$ arrives during the $(k-1)^{\text{st}}$ sampling interval; and *Case 2*: $(\Theta_{ca}^{k-1} + \Delta_s) \ge T$, i.e., $u_{k-1}$ arrives during the $k^{\text{th}}$ sampling intervals.

1. If $\delta_{sc}^k < \Delta_s$ and $(\theta_{ca}^k + \Delta_s) < T$, then

$$\Phi'_k := \begin{cases} [{}^0\phi(T-\varphi_0)\,{}^0D\,{}^0S_2\,{}^0\phi(\varphi_0)\ S_1] & \text{for } (\Theta_{ca}^{k-1}+\Delta_s)<T \\ [{}^0\phi(T-\varphi_0)\ {}^0D\,{}^0S_2\ {}^0\phi(\varphi_0-\varphi_1)\,{}^1\phi(\varphi_1)S_1] & \text{for } (\Theta_{ca}^{k-1}+\Delta_s)\ge T \end{cases}$$

2.If $\delta_{sc}{}^k \ge \Delta_s$ and $\phi_{ca}^k + \Delta_s < T$, then

$$\Phi'_k := \begin{cases} [{}^0\phi(T-\varphi_0)\,{}^1D\,{}^1S_2\,{}^0\phi(\varphi_0)\ S_1] & \text{for } (\Theta_{ca}^{k-1}+\Delta_s)<T \\ [{}^0\phi(T-\varphi)_0\ {}^1D\,{}^1S_2^0\ \phi(\varphi_0-\varphi_1)\,{}^1\phi(\varphi_1)S_1] & \text{for } (\Theta_{ca}^{k-1}+\Delta_s)\ge T \end{cases}$$

3. If $\delta_{sc}^k < \Delta_s$ and $\phi_{ca}^k + \Delta_s \ge T$, then

$$\Phi'_k := \begin{cases} [{}^0D\,{}^0S_2\,{}^0\phi(T)S_1] & \text{for } (\Theta_{ca}^{k-1}+\Delta_s)<T \\ [{}^0D\,{}^0S_2\,{}^0\phi(T-\varphi_1)\ {}^1\phi(\varphi_1)S_1 & \text{for } (\Theta_{ca}^{k-1}+\Delta_s)\ge T \end{cases}$$

4. If $\delta_{sc}^k \ge \Delta_s$ and $\Theta_{ca}^k + \Delta_s \ge T$, then

$$\Phi'_k := \begin{cases} [{}^1D\,{}^1S_2\,{}^0\phi(T)S_1] & \text{for } (\Theta_{ca}^{k-1}+\Delta_s)<T \\ [{}^1D\,{}^1S_2\,{}^0\phi(T-\varphi_1)\ {}^1\phi(\varphi_1)S_1 & \text{for } (\Theta_{ca}^{k-1}+\Delta_s)\ge T \end{cases}$$

where $\varphi_0 := (\Theta_{ca}^k + \Delta_s)$ and $\varphi_1 := (\Theta_{ca}^{k-1} + \Delta_s - T)$.

*Remark 5:* Using the method of event sequencing and notations used by Ray and Halevi [1, 2], the expressions in the above four scenarios can be denoted in a single compact form as:

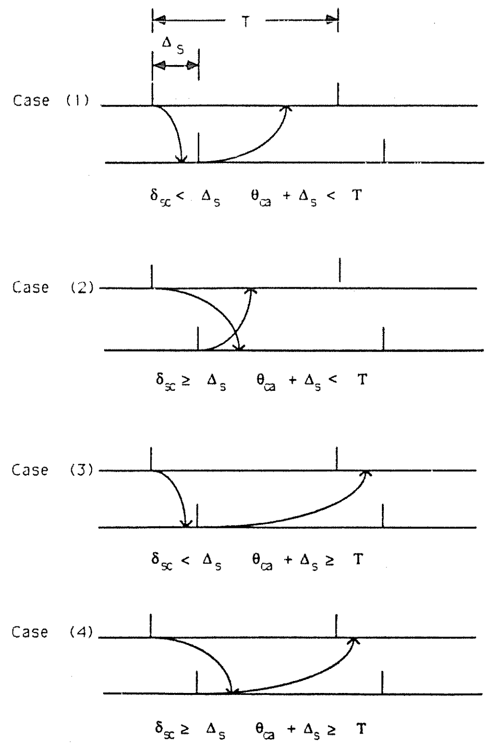


**Fig. 3 Timing diagrams for different delay scenarios**

$$\Phi_k' := [{}^0\phi(T-t_0)\ {}^{p(k)}D\ {}^{p(k)}S_2\ {}^0\phi(t_0-t_1)\ {}^1\phi(t_1)\ S_1]$$

where

$$t_0 := \begin{cases} (\Theta_{ca}^k + \Delta_s) & \text{for } (\Theta_{ca}^{k-1} + \Delta_s) < T \\ T & \text{for } (\Theta_{ca}^{k-1} + \Delta_s) \geq T \end{cases}$$

$$t_1 := \begin{cases} (\Theta_{ca}^{k+1} + \Delta_s - \mathrm{T}) & \text{for } (\Theta_{ca}^{k-1} + \Delta_s) \geq T \\ 0 & \text{for } (\Theta_{ca}^{k-1} + \Delta_s) < T \end{cases}$$

and $p(k) \in \{0,1\}$ is the number of samples by which sensor data is delayed at the controller before being processed. ■

The above observation is valid for the simple case of $\delta_{sc}$ and $\delta_{ca}$ being bounded by $T$. If this restriction is relaxed by increasing the respective upper bounds to $\mathfrak{p}T$ and $\ell T$, respectively, as seen in [1], then the augmented state $X_k$ will include the additional terms, $u_{k-1}, \ldots, u_{k-\ell}, y_{k-1}, \ldots, y_{k-\mathfrak{p}}$. Consequently, $\ell$ or $\mathfrak{p}$ additional versions of sub-state-transition matrices will have to be generated for the Sample and Hold, discrete dynamic, and continuous dynamic elements.

The discussion above evinces that the modeling notation and bookkeeping become quite cumbersome if Kalman and Bertram's approach is used for modeling of *ICCS*. Furthermore, since $\Phi_k'$ is obtained by multiplication of a number of sub-state-transition matrices, it is difficult to assess the impact of changes in data latencies on the overall system. In contrast, Ray and Halevi's approach shows how the individual elements of $\Phi_s'$ are directly influenced by data latencies.

If the sensor and controller sampling rates are nonidentical, i.e., $T_s \neq T_c$, then the system belongs to the class of multi-rate sampling [3]. Ritchey and Franklin [4] have used Kalman and Bertram's approach to model multi-rate systems for stability analysis in the absence of any induced delays. In a recent publication [5], we have used Ray and Halevi's approach to model mutli-rate systems for both zero and non-zero induced delays. The results in Sections 2.1 and 2.2 of [5] show that, even moderate data latencies (i.e., $\delta_{sc}$ and $\delta_{ca}$ being bounded by their respective sampling periods) render the task of multi-rate system modeling much more complex than that for $T_s = T_c$. Although the above approach should yield results similar to Ritchey and Franklins's [4] in the absence of induced delays, the task of book-keeping needed to keep track of varying delays at every sample is expected to be much more cumbersome for modeling multirate systems if Kalman and Bertram's approach [3] is used instead of that in [5].

## 4 Conclusions

Although Kalman and Bertram's approach [3] provides a unified procedure for modeling digital systems, it becomes cumbersome when varying delays are introduced within the control loop. Finite-dimensional modeling of systems with distributed and varying delays, especially developed for Integrated Communication and Control systems (*ICCS*) [1, 2, 5] provides an invariant model structure, simplicity and brevity of notations, fewer matrix multiplications, and more direct insight into the impact of induced delays on the system dynamics, i.e., the state transition and input matrices.

## References

1 Halevi, Y., and Ray, A., "Integrated Communication and Control Systems: Part I—Analysis," ASME Journal of Dynamic Systems, Measurement and Control, Dec. 1988, pp. 367-373.

2 Ray, A., and Halevi, Y., "Integrated Communication and Control Systems: Part II—Design Considerations," ASME Journal of Dynamic Systems, Measurement, and Control, Dec. 1988, pp. 374-381.

3 Kalman, R. E., and Bertram, J. E., "A Unified Approach to the Theory of Sampling Systems," *Journal of Franklin Institute*, Vol. 267, 1959, pp. 405-436.

4 Ritchey, V. S., and Franklin, G. F., "A Stability Criterion for Asynchronous Multirate Linear Systems," *IEEE Trans. on Automatic Control*, Vol. 34, No. 5, May 1989, pp. 529-535.

5 Liou, L-W., and Ray, A., "Integrated Communication and Control Systems: Part III — Non-identical Sensor and Controller Sampling," ASME Journal of Dynamic Systems, Measurement, and Control, Sept. 1990.

# On Linearized Coefficients for an Underlapped Servo-Valve Coupled to a Single-Rod Cylinder

J. Watton[1]

### Nomenclature

$a_1, a_2$ = linearized coefficient factors
$A_1, A_2$ = cylinder area and annulus area
$F, \bar{F}$ = cylinder load force and nondimensional value $F/P_sA_2$
$G_a$ = servoamplifier gain
$H_p$ = position transducer gain
$i$ = servoamplifier current
$i_u$ = servoamplifier current to open servovalve spool to the underlap boundary
$K_i$ = flow coefficient $k_f\sqrt{P_s}$
$k_f$ = servovalve flow constant
$K_p$ = system open-loop gain term $\dfrac{G_aH_pk_f\sqrt{\dfrac{P_s}{2}}}{A_2}$
$P_1, P_2$ = line pressures
$P_s$ = supply pressure
$Q_1, Q_2$ = line flow rates
$R_u$ = servovalve resistance $\sqrt{2P_s}/k_fi_u$
$U$ = cylinder velocity
$y$ = position
$\alpha$ = system open-loop gain factor
$\gamma$ = cylinder area ratio $A_1/A_2$

### Introduction

A linearized analysis is commonly used in the study of electrohydraulic systems to determine appropriate defining transfer functions. These transfer functions may then be used to obtain a feel for dynamic performance as a first step towards system design [1-4]. The servovalve nonlinear flow characteristic has therefore to be linearized, which results in the derivation of flow and pressure coefficients. The purpose of this note is to show that these coefficients are functions of the cylinder area ratio as well as the load force for a position

[1]Department of Mechanical Engineering and Energy Studies, University College Cardiff, Cardiff, U.K.

Contributed by the Dynamic Systems and Control Division of The American Society of Mechanical Engineers. Manuscript received by the Dynamic Systems and Control Division July 1988; revised manuscript received August 1989. Associate Editor: D. Hullender.